Dissolution and reprecipitation of carbonitride precipitates in carbon steel by low-dose α bombardment

1989 J. Phys.: Condens. Matter 1 8799

(http://iopscience.iop.org/0953-8984/1/45/005)

J. Phys.: Condens. Matter 1 (1989) 8799–8808. Printed in the UK

Dissolution and reprecipitation of carbonitride precipitates in carbon steel by low-dose α bombardment

S M M Ramos, L Amaral, M Behar, G Marest†, A Vasquez and F C Zawislak

Instituto de Fisica, Universidade Federal do Rio Grande do Sul, 91500 Porto Alegre, RS, Brazil

Received 22 August 1988, in final form 16 March 1989

Abstract. The effects of α post-bombardment on the dissolution and reprecipitation of carbonitrides present in N_2^+-implanted 1020 low-C steel are investigated. The characterisation of the precipitates is done via conversion electron Mössbauer spectroscopy. Our results show that the irradiation of the sample with low-fluence He^+ ions produces dissolution of the ε-$Fe_{3,2}(C, N)$ and reprecipitation into ε-$Fe_{2+x}(C, N)$ ($x < 1$). It is also shown that the dissolution and reprecipitation mechanism is strongly dependent on the type of precipitate present in the sample. Finally it is shown that the presence of He^+ atoms in the implanted region raises the temperature at which the precipitates remain stable.

1. Introduction

The implantation of N_2^+ into Fe and steels induces the formation of nitride and carbonitride precipitates in the implanted layer ([1–3] and references therein). It is now well established that the presence of these precipitates improves considerably the tribological properties of the implanted steels. As a consequence, during the last few years, considerable effort has been devoted to the study of the various parameters (implanted dose, temperature of implantation, composition of the alloy, thermal treatment, etc) which can affect the tribological properties of implanted Fe or steel [4].

On the contrary, the influence of ion post-bombardment on the formation and thermal evolution of carbonitride precipitates has received much less attention. It is known that the thermodynamic stability of an alloy containing precipitates can be modified by ion bombardment. The irradiation can produce both dissolution of precipitates and their reprecipitation, as well as other effects. Ion bombardment changes not only the composition of the precipitates but also its thermal behaviour. This kind of effect has been widely studied for coherent precipitates in austenitic steels [5] as well as in Fe and Ni alloys, where complex phase transitions have been observed [6].

In [7] the effect of α post-bombardment on nitride precipitates formed by N_2^+ implantation into Fe foils was recently investigated. This work has shown that bombardment not only produces partial dissolution of the nitrides but also affects their thermal evolution. The same work shows that the influence of the α bombardment strongly depends on the type of pre-existing N precipitates. A natural extension of these findings is to

† Permanent address: Institut de Physique Nucléaire, Université Claude Bernard, Lyon, France.

0953-8984/89/458799 + 10 $02.50

investigate the influence of α post-bombardment on nitrides and carbonitrides formed by controlled N_2^+ implantation into different kinds of steel.

In this work, we present a detailed study of N_2^+-implanted 1020 low-C steel. The analysis of the results, obtained through conversion electron Mössbauer spectroscopy (CEMS) shows that the post-irradiation of the sample with He^+ ions can produce dissolution and reprecipitation of the carbonitride compounds. Finally it is shown that the retention of the carbonitride precipitates is affected by the presence of He atoms and depends on the thermal history of the sample.

2. Experimental details

Samples obtained from industrial ingots of 1020 low-C steel (containing 0.2 wt% C and 0.9 wt% Mn) were mechanically polished and implanted at the HVEE 400 keV ion implanter of the Institute of Physics, Porto Alegre. The N_2^+ ions have been implanted at 140, 80 and 40 keV in order to obtain a plateau in the ion distribution from the surface up to approximately 1200 Å. Typical doses were 6×10^{16} N_2^+ cm^{-2} and the N concentration at the plateau was around 40 at.%. The α post-bombardment was carried out at two different energies: the first at 25 keV, which leaves the He^+ ions in the N_2^+-implanted region ($R_p = 800$ Å; $\Delta R_p = 650$ Å); the second at 150 keV ($R_p = 2600$ Å), leaving the He^+ ions outside the N_2^+-implanted area. The sample implanted with 25 keV α-particles was studied as a function of the fluence in the range from 10^{14} to 1.4×10^{16} α cm^{-2}. For the 150 keV energy sample the fluence φ was fixed at 7×10^{15} α cm^{-2}. The current density during the implantations of N_2^+ and He^+ was always less than 1 μA to avoid excessive heating of the samples (always below 50 °C).

Two types of N_2^+-implanted sample were studied. One type, which was first annealed at 400 °C and then bombarded, will be referred to as the [1020 N_2^+ (400, α)] sample. The other, which is first bombarded and then annealed at the same temperature, will be referred to as the [1020 N_2^+ (α, 400)] sample. These and further anneals were performed in a vacuum of better than 10^{-6} Torr at the specified temperatures for 1 h each. The implanted samples were analysed by the CEMS technique using a ^{57}Co–Rh source probing a region which coincides with the N_2^+-implanted zone. The CEMS detector operates with a continuous gas flux of He–CH_4. The measurements were obtained by means of a conventional Mössbauer set-up operating in the constant-acceleration mode. The data were stored and analysed using specially designed software to operate in an IBM PC type microcomputer.

3. Results

The measured CEMS spectra for the various samples and temperatures are shown in figures 1–4. The Mössbauer hyperfine parameters obtained in the analysis of our data are given in table 1. Tables 2–4 display the normalised CEMS spectrum areas for the martensitic and the carbonitride precipitates present in the samples at various stages of the experiment.

3.1. The [1020 N_2^+ (α, 400)] sample

The CEMS spectrum of the N_2^+-implanted sample in figure 1, presents in addition to the characteristic sextet of the martensitic steel, a quadrupole doublet typical of ξ- or

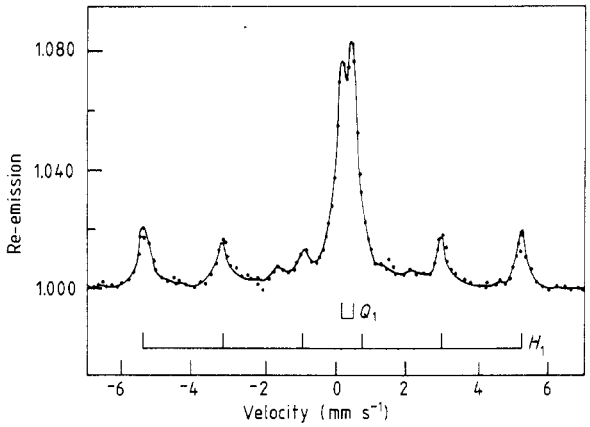

Figure 1. ^{57}Fe CEMS spectrum measured at room temperature for 1020 steel implanted with N_2^+: ———, least-squares fit to the experimental data. H_1 is the magnetic field characteristic of the steel matrix and Q_1 the nuclear quadrupole splitting of ε-$Fe_2(C, N)$. In addition there is a small contribution due to θ-$Fe_3(C, N)$, a hyperfine field which is not indicated in the figure.

Table 1. ^{57}Fe Mössbauer parameters obtained from the least-squares fit to the present data. H_1, H_2, H_3 and H_4 are the sets of characteristic magnetic fields corresponding to Fe, ε-$Fe_{2+x}(C, N)$, ε-$Fe_{3.2}(C, N)$ and θ-$Fe_3(C, N)$, respectively, and Q_1 and Q_2 are the characteristic quadrupole splittings corresponding to ε-$Fe_2(C, N)$ and ε-$Fe_{2+x}(C, N)$. The isomer shift δ is given relative to Fe metal at room temperature.

	H (kG)		E_0 (mm s^{-1})	δ (mm s^{-1})
Fe	331 ± 3	H_1		0.01 ± 0.02
ε-$Fe_{2+x}(C, N)$	279 ± 4	H_2		0.27 ± 0.05
	218 ± 4	H_2		0.25 ± 0.02
	133 ± 5	H_2	−0.06 ± 0.02	0.43 ± 0.04
		Q_2	0.76 ± 0.02	0.36 ± 0.02
ε-$Fe_{3.2}(C, N)$	238 ± 3	H_3		0.31 ± 0.02
	298 ± 3	H_3		0.24 ± 0.04
θ-$Fe_3(C, N)$	198 ± 5	H_4		0.45 ± 0.02
ε-$Fe_2(C, N)$		Q_1	0.32 ± 0.02	0.40 ± 0.02

ε-$Fe_2(C, N)$ [8, 9] plus a minor contribution of θ-$Fe_3(C, N)$. It is known that the ξ-Fe_2N, ε-Fe_2N or ε-$Fe_2(C, N)$ precipitates have similar crystalline structures and therefore give almost identical Mössbauer parameters. However, results of glancing x-ray diffraction measurements performed on similar systems [3] have shown that C steels implanted with N_2^+ led to the formation of carbonitrides. Moreover, it was argued in [10] and [11] that this situation occurs whenever a N_2^+ implantation is performed on a C steel. Therefore in what follows we are going to assume that the present N_2^+ implantations have produced carbonitrides rather than nitrides.

The 25 keV, $\varphi = 7 \times 10^{15}$ α cm^{-2} bombardment does not produce any modification in the CEMS spectrum shown in figure 1, meaning that there is no evidence of precipitate

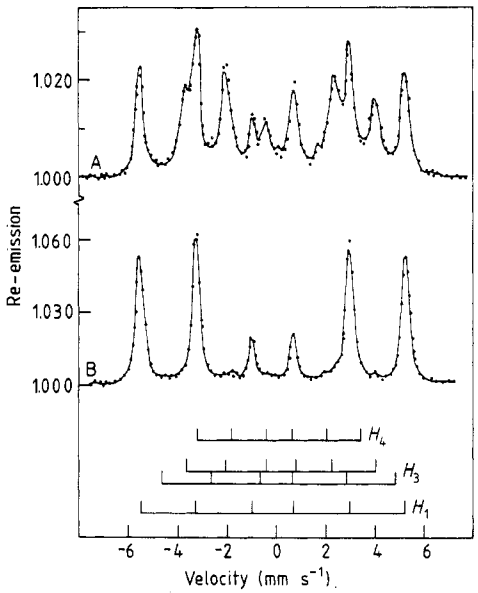

Figure 2. ^{57}Fe CEMS spectra measured at room temperature: spectrum A, [1020 N_2^+ (α, 400)] sample after α implantation and subsequent annealing at 400 °C; spectrum B, same sample after additional annealing at 450 °C. H_1 represents the magnetic field of the 1020 steel, H_3 the two magnetic fields of ε-$Fe_{3.2}$(C, N) and H_4 magnetic field corresponding to θ-Fe_3(C, N). All annealing times were 1 h.

Table 2. Normalised CEMS spectral areas of carbonitride precipitates at the annealing temperatures indicated for the sample [1020 N_2^+ (α, 400)]. Typical errors are 5%, and annealing times 1 hr.

	Normalised spectral area			
	Fe	ε-Fe_2(C, N)	θ-Fe_3(C, N)	ε-$Fe_{3.2}$(C, N)
As implanted	0.33	0.63	0.04	—
α (25 keV) bombarded	0.33	0.63	0.04	—
Annealed at 400 °C	0.44	—	0.07	0.49
Annealed at 450 °C	0.95	—	—	0.05
Annealed at 500 °C	1.00	—	—	—

dissolution. The subsequent annealing of the sample at 400 °C produced complete transformation of ε-Fe_2(C, N) into ε-$Fe_{3.2}$(C, N) as shown in figure 2, spectrum A. Thus, the annealing results in a redistribution of N_2^+ in the implanted zone, involving the formation of less dense carbonitride precipitates. At this stage a significant part (49%) of the total CEMS area corresponds to ε-$Fe_{3.2}$(C, N) (see table 2). Further annealing at 450 °C drastically reduces the concentration of the precipitates to only 5%. Finally, annealing at 500 °C dissolves all carbonitrides as shown by the corresponding CEMS spectrum (figure 2, spectrum B).

3.2. The [1020 N_2^+ (400, α)] sample

The 400 °C anneal of the N_2^+-implanted sample before He^+ implantation shows the same effect as observed for the [1020 N_2^+ (α, 400)] sample, annealed after He^+ implantation: dissolution of the ε-Fe_2(C, N) precipitate and its transformation to ε-$Fe_{3.2}$(C, N) (see figure 3 and table 3).

The 25 keV, $\varphi = 7 \times 10^{15}$ $\alpha\,cm^{-2}$ post-bombardment alters the CEMS spectrum drast-

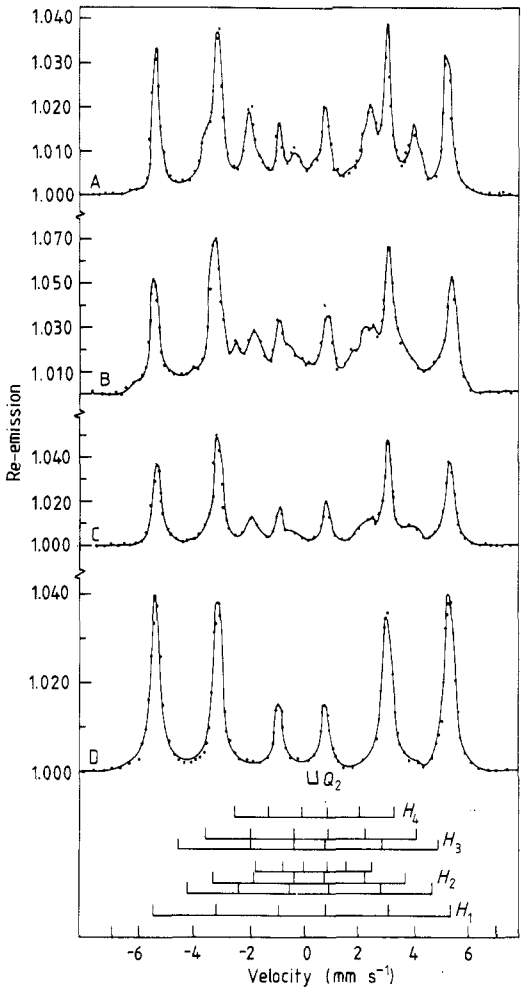

Figure 3. ^{57}Fe CEMS spectra measured at room temperature: spectrum A, sample in figure 1 after annealing at 400 °C; spectrum B, [1020 N_2^+ (400, α)] sample after annealing at 400 °C and subsequent α implantation; spectrum C, [1020 N_2^+ (400, α)] sample after additional annealing at 450 °C; spectrum D, sample [1020 N_2^+ (400, α)] after additional annealing at 500 °C. H_1, H_3 and H_4 are defined in figure 2. H_2 corresponds to the three magnetic fields of ε-Fe_{2+x}(C, N). Q_2 corresponds to the nuclear quadrupole splitting of ε-Fe_{2+x}(C, N). All annealing times were 1 h.

Table 3. Normalised CEMS spectral areas of carbonitride precipitates at the annealing temperatures for the [1020 N_2^+ (400, α)] sample. Typical errors are 5% and annealing times 1 h.

	Normalised spectral area				
	Fe	ε-Fe_2(C, N)	ε-Fe_{2+x}(C, N)	θ-Fe_3(C, N)	ε-$Fe_{3.2}$(C, N)
As implanted	0.33	0.63		0.04	
Annealed at 400 °C	0.47			0.07	0.46
α (25 keV) bombarded	0.50	—	0.42	0.08	—
Annealed at 450 °C	0.75	—	—	0.05	0.20
Annealed at 500 °C	1.00	—	—	—	—
α (150 keV) bombarded	0.60	—	0.35	0.05	—
Annealed at 450 °C	1.00	—	—	—	—

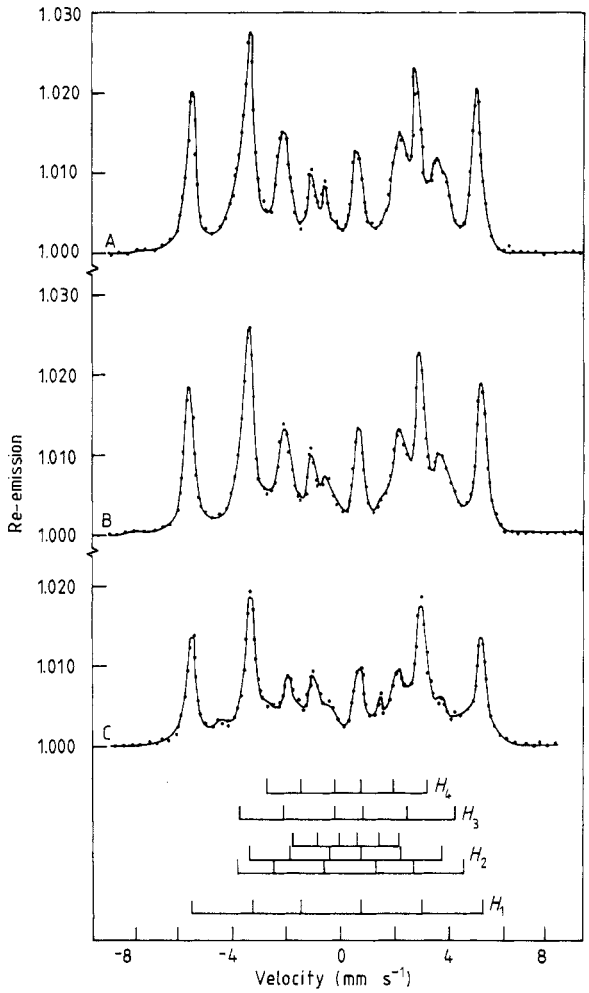

Figure 4. ^{57}Fe CEMS spectra measured at room temperature for the [1020 N_2^+ (400, α)] sample irradiated with different α fluences: spectrum A, $\varphi = 10^{14}$ α cm^{-2}; spectrum B, $\varphi = 6 \times 10^{14}$ α cm^{-2}; spectrum C, $\varphi = 3.5 \times 10^{13}$ α cm^{-2}. The magnetic fields H_1, H_2, H_3 and H_4 are defined in figures 2 and 3.

ically, as shown in figure 3, spectrum B. Analysis of the spectrum indicates complete dissolution of ε-$Fe_{3.2}(C, N)$ and its reprecipitation into ε-$Fe_{2+x}(C, N)$ [3, 12] with $x < 1$. At this stage a small quantity of θ-$Fe_3(C, N)$ remains, the total contribution of the carbonitrides to the CEMS spectrum being relatively high (50%; see table 3).

Annealing at 450 °C produces transformation of ε-$Fe_{2+x}(C, N)$ and θ-$Fe_3(C, N)$ to ε-$Fe_{3.2}(C, N)$ as shown in figure 3, spectrum C. At this point, ε-$Fe_{3.2}(C, N)$ is still a significant part of the total CEMS area (20%). Finally, after annealing at 500 °C, the CEMS spectrum in figure 3, spectrum D, shows only the characteristic sextet corresponding to martensitic steel, indicating dissolution of the carbonitrides.

In order to follow the transformation of ε-$Fe_{3.2}(C, N)$ to ε-$Fe_{2+x}(C, N)$, we have increased the dose φ from 10^{14} α cm^{-2} to 1.4×10^{16} α cm^{-2}. The results are displayed in figure 4 and table 4. At the lowest dose (10^{14} α cm^{-2}), ε-$Fe_{3.2}(C, N)$ has already partially reprecipitated into ε-$Fe_{2+x}(C, N)$. By increasing the dose, the amount of ε-$Fe_{3.2}(C, N)$ decreases and the amount of ε-$Fe_{2+x}(C, N)$ increases. Finally for 3×10^{15} α cm^{-2} the reprecipitation process is completed. Further irradiation, up to 1.4×10^{16} α cm^{-2}, does not cause any change in the concentration of ε-$Fe_{2+x}(C, N)$.

Table 4. Normalised CEMS spectral areas of carbonitride precipitates at different α fluences (E_α = 25 keV) for the 1020 N_2^+ (400, α) sample. Typical errors are 5%.

	Normalised spectral area for the following fluences			
	10^{14} $\alpha\,cm^{-2}$	6×10^{14} $\alpha\,cm^{-2}$	3.5×10^{15} $\alpha\,cm^{-2}$	1.4×10^{16} $\alpha\,cm^{-2}$
Fe	0.50	0.50	0.50	0.50
ε-$Fe_{2+x}(C, N)$	0.24	0.36	0.43	0.43
ε-$Fe_{3.2}(C, N)$	0.20	0.07	—	—
θ-$Fe_3(C, N)$	0.06	0.07	0.07	0.07

In the next step we increased E_α in order to leave the He^+ atoms outside the N_2^+-implanted region. To achieve this, we bombarded the sample annealed at 400 °C with E_α = 150 keV and $\varphi = 7 \times 10^{15}$ $\alpha\,cm^{-2}$. The effect of this irradiation is the same as that performed with E_α = 25 keV; there is complete transformation of the ε-$Fe_{3.2}(C, N)$ to ε-$Fe_{2+x}(C, N)$ precipitates, as shown in table 3. However, after further annealing at 450 °C the CEMS spectrum shows only the characteristic lines of martensite.

4. Discussion

Our experimental results show that the precipitates produced by implanting N_2^+ into a 1020 low-C steel are affected by post-bombardment mainly in two ways: firstly, modification of the thermal behaviour of the precipitates; secondly, dissolution and reprecipitation of the carbonitrides. In what follows, we discuss these effects separately.

4.1. Thermal behaviour of the precipitates

In [13] it was found that ε-$Fe_{3.2}(C, N)$ obtained by N_2^+ implantation into 1020 steel are stable up to 400 °C. For higher temperatures, they dissolve as a consequence of N diffusion out of the implanted region. The results of the present work show that the presence of He atoms in the N_2^+-implanted region inhibits N diffusion, resulting in the retention of precipitates at higher temperatures. This statement is supported by the following features. First, when the [1020 N_2^+ (400, α)] sample is bombarded at E_α = 25 keV and then annealed at 450 °C, it retains a considerable quantity of ε-$Fe_{3.2}(C, N)$ precipitates. However, when the α implantation energy is increased to 150 keV (R_p outside the carbonitride region), the further anneal at 450 °C results in complete dissolution of the precipitates. Secondly, after annealing at 400 °C, the [1020 N_2^+ (α, 400)] sample became richer in carbonitrides than the sample which was first N_2^+ implanted and then annealed, i.e. the [1020 N_2^+ (400, α)] sample (see table 4). This should be attributed to the retentive action of the He atoms only present during the annealing of the first sample.

These facts can be understood by taking into account the well known behaviour of He atoms implanted into metals. He can accumulate in large quantities in metals and alloys. The accumulation occurs through the creation of vacancies during the implantation process which stabilises He via the formation of He_n–V_m complexes ([14, 15] and references therein). At room temperature and for low implantation doses (as in the present case) the α-irradiation induces small He–V complexes which are finely

dispersed. However, for increasing temperature and/or He dose, the He–V complexes grow in size and eventually form He bubbles [14]. The above mechanisms can be associated with the retention effect observed in the present experiment. The implanted α-particles create He_n–V_m complexes which end up at grain boundaries and precipitates. When the anneal is performed, two competitive effects can occur. First, the He_n–V_m complexes will act as agglomeration centres for the N released from precipitates. This prevents N from migrating very far, favouring the observed retention effect. It should be pointed out that He–N-trapping effects have already been observed in He profiling experiments [16]. Secondly, the same annealing process will favour the agglomeration of the He–V complexes, which will become larger, less disperse and therefore less efficient in the N-trapping mechanism.

The bombardment of [1020 N_2^+ (400, α)] with particles produces $Fe_{2+x}(C, N)$. This is similar in structure to the ε-$Fe_{3.2}(C, N)$, differing only in the size of the parameters of the hexagonal close-packed (HCP) unit cell. By comparing the Mössbauer parameters obtained in the present work, with those in [12] from measurements on carbonitride powders, we conclude that in our case $0.55 \leqslant x \leqslant 0.66$. The difference between the sizes of the corresponding unit cells is only 3%. This difference is not significant and cannot account for the difference between the thermal behaviours of the precipitates.

After annealing at 450 °C, the [1020 N_2^+(400, α)] sample became richer in carbonitrides than the (1020 N_2^+(α, 400)] sample. This difference could be tentatively attributed to the thermal evolution of the He_n–V_m complexes rather than to the precipitates present during the annealing process (ε-$Fe_{2+x}(C, N)$ and ε-$Fe_{3.2}(C, N)$, respectively). In fact, in the first case ([(1020 N_2^+(400, α)] sample), the He_n–V_m complexes are submitted to one annealing process. Instead, in the second case ([(1020 N_2^+(α, 400)] sample), they are submitted to successive anneals at 400 and 450 °C; then the complexes agglomerate and become less efficient in N trapping.

In the work in [7], N_2^+ has been implanted into pure Fe, α post-bombarded and annealed under the same conditions and sequences as in the present experiment, giving as the final products γ-Fe_4N and ε-$Fe_{3.2}N$ precipitates which were retained up to 500 °C. In the present case the [1020 N_2^+(α, 400)] sequence retained ε-$Fe_{3.2}(C, N)$ only up to 450 °C whereas in the work in [7] the same sequence retained 6% of ε-$Fe_{3.2}N$ and 22% of γ-Fe_4N at the higher temperature of 500 °C. The observed differences between the types and thermal behaviours of the precipitates should be attributed to the different compositions of the implanted samples (the Fe in [7] was C free, and the 1020 sample in our work has a low C concentration). This conclusion is based on previous work in which it was noticed that the pre-existing structure has a strong influence on the formation and thermal behaviour of nitrides and/or carbonitrides [10, 11].

The conclusion from both experiments is that the presence and thermal evolution of the He_n–V_m complexes and the composition of the implanted sample play a significant role in the retention process of the nitride and carbonitride precipitates.

4.2. Dissolution of the precipitates

Our work shows that the different kinds of carbonitride formed in the 1020 steel after N_2^+ implantation behave differently under bombardment. The ε-$Fe_2(C, N)$ precipitates have proved to be very stable under light-particle irradiation. The α bombardment produced neither partial dissolution nor reprecipitation into other kinds of carbonitride. Even for an α dose as high as 10 displacements/atom (dpa) we have not observed any trace of ε-$Fe_2(C, N)$ dissolution.

Table 5. Normalised CEMS subspectral areas corresponding to one, two and three (C, N) NNs to Fe atoms at different α fluences (E_α = 25 keV). Typical errors are of the order of 2%.

	Normalised subspectral area for the following fluences							
	10^{14} α cm^{-2}	6×10^{14} α cm^{-2}	9×10^{14} α cm^{-2}	3.5×10^{15} α cm^{-2}	5×10^{15} α cm^{-2}	7.5×10^{15} α cm^{-2}	9×10^{15} α cm^{-2}	1.4×10^{16} α cm^{-2}
$H_2^1 = 279$ kG	—	—	—	0.09	0.11	0.12	0.14	0.16
$H_2^2 = 218$ kG	0.25	0.23	0.21	0.19	0.16	0.15	0.14	0.11
$H_2^3 = 133$ kG	—	0.13	0.14	0.15	0.17	0.16	0.17	0.16

On the contrary, the ε-$Fe_{3.2}(C, N)$ precipitates have been shown to be unstable under α bombardment. For an irradiation dose φ as low as 10^{14} α cm^{-2} (0.1 dpa) they partially reprecipitate into ε-$Fe_{2+x}(C, N)$, the transformation being complete after $\varphi = 3.5 \times 10^{15}$ α cm^{-2}.

It has been shown [17] that in the HCP carbonitride structure the C and N atoms are interstitial near neighbours (NNs) to the Fe atoms. In particular for the ε-Fe_{2+x} phase the magnetic hyperfine field corresponding to one, two and three C or N NNs are, respectively, $H_2^1 = 279$ kG, $H_2^2 = 218$ kG and $H_2^3 = 133$ kG [12]. Therefore from the Mössbauer pattern and the resonant areas of each subspectrum it is possible to assign the population corresponding to the different NN configurations. In table 5 they are shown as a function of the α implantation dose. It can be observed that on increasing the dose the second-NN population decreases from about 25% to 11%. The third-NN population which is zero at $\varphi = 10^{14}$ α cm^{-2} increases to 15% for $\varphi = 3.5 \times 10^{15}$ α cm^{-2} and then remains approximately constant. Finally, the first-NN population, which is also zero up to $\varphi = 3.5 \times 10^{15}$ α cm^{-2}, starts to increase steadily with increasing dose. Therefore, one can conclude that the α post-bombardment not only produces the ε-$Fe_{3.2}(C, N)$ dissolution but also changes the relative (C, N) NN population in ε-$Fe_{2+x}(C, N)$.

Finally it should be mentioned that the ε-Fe_2N and γ-Fe_4N produced in Fe suffered [7] only partial dissolution after 1 dpa α bombardment. No reprecipitation process has been observed. These results are at variance with the present ones where, firstly, the ε-$Fe_2(C, N)$ has not been dissolved even after a 10 dpa bombardment dose and, secondly, a reprecipitation ε-$Fe_{3.2}(C, N) \rightarrow \varepsilon$-$Fe_{2+x}(C, N)$ process has been observed. All these arguments indicate that the sample composition plays an important role in the dissolution and/or reprecipitation process under α bombardment.

To our knowledge, this is the first detailed study of reprecipitation and dissolution of carbonitrides (produced by implantation) as a consequence of light-ion bombardment. On the contrary, extensive work has been performed to study the stability mainly of coherent precipitates under neutron and heavy-particle irradiation. In particular in [18] by self-ion irradiating Al–Mg–Si alloys the microstructural changes were followed as a function of the irradiation dose. It was found that, irrespective of the alloy chemistry or irradiation conditions, the precipitate interface is considerably modified under irradiation. It was argued that the loss (or modification) of the interfacial dislocations (which obstruct the dissolution) marks the beginning of the rapid dissolution of the precipitates. Based on these observations, the stability of the precipitates during the irradiation was attributed to the presence of the interfacial dislocations.

At present, we do not have a plausible explanation for the behaviour observed in our work. Very tentatively we can assume that the mechanism proposed in [18] may also be valid in the present case.

The main difference between our work and the results in [18] is that we observe dissolution and reprecipitation under irradiations by He^+, a very light projectile compared with the 250 keV, Ni and Al used in the work in [18]. This means that we produce much less nuclear damage. In our experiments, we have typically 0.7 dpa compared with about 10 dpa in [18].

5. Conclusions

The present work has shown that the precipitates produced by N_2^+ implantation into 1020 steel are affected by α post-bombardment in two ways.

First, we observed dissolution and reprecipitation of the carbonitrides. It is shown that the ε-$Fe_{3.2}(C, N)$ precipitates are highly unstable under particle bombardment, dissolving at rather low implantation dose. On the contrary, ε-$Fe_2(C, N)$ is very stable, showing no trace of dissolution process even at doses as high as 1.4×10^{16} α cm^{-2} (10 dpa).

Secondly, the presence of He atoms in the N_2^+-implanted region has modified the thermal behaviour of the carbonitrides. While the unimplanted samples retain precipitates up to 400 °C, the presence of He atoms in the implanted region raises this temperature to 450 °C. This phenomenon is attributed to the He_m–V_n complexes that agglomerate at the grain boundaries of the precipitates, inhibiting N diffusion.

Finally it is shown that the trapping efficiency strongly depends on the kinds of precipitates involved in the process as well as on the composition of the matrix where the precipitates are formed. This retention effect could be of potential technological application in metallurgy, where retention of protective carbonitrides is of major importance.

References

[1] Longworth G and Hartley E W 1978 *Thin Solid Films* **48** 95
[2] dos Santos C A, de Barros B A S Jr, de Souza J P and Baumvol I J R 1982 *Appl. Phys. Lett.* **41** 237
dos Santos C A 1985 *PhD Thesis* Universidade Federal Rio Grande do Sul
[3] Marest G 1988 *Ion Implantation 1988* ed. F H Wohlbier (Aldermannsdorf: Trans Tech)
[4] Herman H 1982 *Nucl. Instrum. Methods* **182–3** 887
[5] Nelson R S, Hudson J A and Mazey D Y 1972 *J. Nucl. Mater.* **44** 318
[6] Farrel K, Maziasz P J, Lee E H and Mansur L K 1983 *Radiat. Eff.* **78** 227
[7] Behar M, Viccaro P J, Silva M T X, Vasquez A, dos Santos C A and Zawislak F C 1987 *Nucl. Instrum. Methods* B **19–20** 132
[8] Chabanel M, Janot C and Motte J P 1968 *C.R. Acad. Sci., Paris* B **266** 419
[9] Jack H 1948 *Proc. R. Soc.* A **195** 34
[10] Principi G, Matteazi P, Ramous E and Longworth G 1980 *J. Mater. Sci.* **15** 2665
[11] dos Santos C A, Behar M and Baumvol I J R 1984 *J. Phys. D: Appl. Phys.* **17** 969
[12] Firrao D, Rosso M, Principi G and Grattini R 1982 *J. Mater. Sci.* **17** 1773
[13] dos Santos C A, Behar M and Baumvol I J R 1984 *J. Phys. D: Appl. Phys.* **17** 551
[14] Ullmaier H 1983 *Radiat. Eff.* **78** 1
[15] Picraux S T 1981 *Nucl. Instrum. Methods* **182–3** 413
[16] Hantala M, Anttila A and Hirvonen I 1987 *Nucl. Instrum. Methods* B **19–20** 50
[17] de Christoforo N and Kaplow R 1977 *Metall. Trans.* A **8** 425
[18] Vaidya W N 1979 *J. Nucl. Mater.* **83** 223